

Research Article

Synthesis and Characterization of Screen Printed $\text{Zn}_{0.97}\text{Cu}_{0.03}\text{O}$ Thick Film for Semiconductor Device Applications

Rayees Ahmad Zargar,¹ Sharief Ud Din Khan,¹ Mohd Shahid Khan,¹
Manju Arora,² and Aurangzeb Khurram Hafiz¹

¹ Department of Physics, Jamia Millia Islamia, New Delhi 110025, India

² CSIR-National Physical Laboratory, Dr. K.S. Krishnan Marg, New Delhi 110012, India

Correspondence should be addressed to Rayees Ahmad Zargar; rayeesphy12@gmail.com

Received 25 August 2014; Accepted 3 November 2014; Published 24 November 2014

Academic Editor: Lorenzo Pavesi

Copyright © 2014 Rayees Ahmad Zargar et al. This is an open access article distributed under the Creative Commons Attribution License, which permits unrestricted use, distribution, and reproduction in any medium, provided the original work is properly cited.

The studies on doped ZnO thick films deposited over large surface area are still a very promising area of research and development. We report characteristic properties of thick film of $\text{Zn}_{0.97}\text{Cu}_{0.03}\text{O}$ prepared by the economic screen printing technique. The film was characterized by XRD, SEM, diffused reflectance, FTIR, and dark resistivity measurement techniques. The XRD and SEM studies revealed polycrystalline, single phase, porous, and granular surface morphology of this Cu doped ZnO thick films. The direct band gap energy of this film determined by diffuse reflectance technique is 3.18 eV. IR transmission spectrum measured in $4000\text{--}600\text{ cm}^{-1}$ region at ambient temperature confirmed the incorporation of Cu^{2+} ions in ZnO lattice. The DC resistivity measurements reveal semiconducting nature of the sample with activation energy of 0.66 eV.

1. Introduction

ZnO is one of the most important extensively studied II-VI semiconducting metal oxide. Thousands of papers are appearing in different journals on this material every year. It has a wide direct band gap of around 3.2–3.37 eV at room temperature which can be tuned in the range 3.0 to 4.0 eV by doping with different metals such as Cd and Mg [1, 2]. ZnO generally exhibits n-type conductivity. It has large exciton binding energy of 60 meV, higher optical gain (320 cm^{-1}) at ambient temperature, and Bohr radius $r_B \sim 1.8\text{ nm}$ which helps in stabilizing excitons both chemically and thermally [3, 4]. Moreover, it is cost effective and environment friendly as compared to other metal oxides. Due to these unique properties, it has been widely used in optoelectronic applications such as solar cells, flat panel displays, and light emitting diodes (LEDs) [5]. The thick films of ZnO are used in many applications in the field of optoelectronics, gas sensing, antibacterial and cancer treatment, and so forth [6, 7].

For highly efficient optoelectronic device applications, it is desirable to reduce or tune the band gap in a broad range

together with precise control of conductivity possessed by the film. The band gap energy of ZnO can be varied by doping it appropriately with metal [8]. Recent investigations on group-IB elements, for example, Cu, Ag, and Au doped ZnO revealed the formation of p-type ZnO with reduced band gap [9, 10]. Among these, Cu is the best choice because the size mismatch between Cu and Zn is the smallest which leads to the lowest formation energy. In addition, electrons can be easily injected from Cu layer to ZnO since there is no barrier to the flow of electrons between Cu and ZnO [11]. Thus, incorporation of Cu and variation in its concentration plays key role in changing the physical properties of ZnO thick films. These doped films have important industrial and domestic applications for detecting hazardous gases including LPG [12, 13].

In the present work, $\text{Zn}_{0.97}\text{Cu}_{0.03}\text{O}$ thick film was prepared by using simple and economic screen printing process [14] and their physical properties were characterized by XRD, SEM, UV-spectroscopy, FT-IR, and dark resistivity analytical techniques.

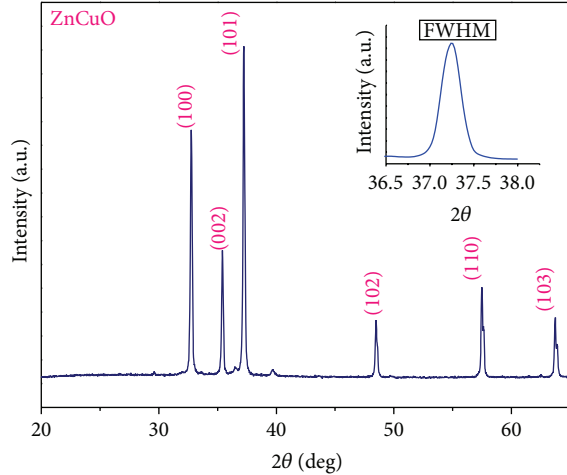


FIGURE 1: XRD diffraction pattern of screen printed $\text{Zn}_{0.97}\text{Cu}_{0.03}\text{O}$ thick film.

2. Materials and Measurements

Thick film paste was prepared by thoroughly mixing AR grade (99.999% purity) ZnO and CuO with anhydrous ZnCl_2 as an adhesive agent, followed by grinding in a mortar and ethylene glycol as a binder. The prepared paste was screen printed on cleaned glass substrates. The glass plates were cleaned with acetone and deionised water for 20 minutes and then dried in hot air over at 60°C for 10 minutes. The as deposited Cu doped ZnO films were heated at 130°C on hot plate for 1 hr for the partial reduction of the solvent and porosity of films [15]. The films were further annealed in a muffle furnace in air at 550°C for ten minutes [16] for proper adherence and stability and for the decomposition of organic materials. The thickness of the film was determined after sintering by weighing method and it was found to be of the order of $14\ \mu\text{m}$.

X-ray diffraction pattern was recorded on advanced Rigaku diffractometer in the 2θ range of 10° – 70° using $\text{Cu-K}\alpha$ X-ray radiation source. The surface morphological information was derived by using scanning electron microscope (SEM, Leo-440, UK) for recording micrographs. FTIR transmission spectrum was recorded by SHIMAZU-8400S, Japan spectrophotometer, in 4000 – $400\ \text{cm}^{-1}$ range at $4\ \text{cm}^{-1}$ resolution. The optical diffused reflectance spectrum was measured on Hitachi make UV-VIS spectrometer-3900 in the 300 – $800\ \text{nm}$ range. DC resistivity measurement was done by using standard four-probe technique.

3. Results and Discussion

3.1. Structural Analysis. To confirm the formation and crystal structure of Cu doped ZnO thick film was examined using powder X-ray diffraction (XRD) technique. The diffraction pattern as well as FWHM curve of (101) plane as inset is shown in Figure 1 and the different parameters calculated are listed in Table 1.

TABLE 1: XRD parameters: d -values (reported and observed), hkl plane, and lattice parameters (a , c) of the $\text{Zn}_{0.97}\text{Cu}_{0.03}\text{O}$ thick film.

hkl plane	d -Value (\AA)		Cell parameters (\AA)	
	Wurtzite structure (hexagonal phase)		a	c
	Reported	Observed		
100	2.81	2.771		
002	2.61	2.581		
101	2.44	2.4279	3.18	5.21
102	1.89	1.876		
110	1.63	1.609		
103	1.46	1.453		

The peak values match well with Wurtzite structure as per (JCPDS) card number 36-1451 [17]. The inset of Figure 1 shows FWHM for the most intense (101) peak to calculate the crystallite size by using Debye-Scherrer's formula [18]:

$$D = \frac{0.9\lambda}{\beta \cos\theta}, \quad (1)$$

where D is the crystallite size (in nm), λ is the X-ray wavelength, β is the width (radians) at half the maximum peak intensity, and θ is the Bragg angle. The estimated value of crystal size comes out to be 30 nm which is in good agreement with earlier result [19].

3.2. SEM Analysis. Figure 2 shows the SEM micrographs of $\text{Zn}_{0.97}\text{Cu}_{0.03}\text{O}$ as deposited thick film under (a) 40000 and (b) 50000 magnification. The SEM images reveal polycrystalline, porous, and interconnected grains surface morphology. The small crystallites agglomerate and form spindle, dumb bell, and cuboidal shaped particles along with fused clusters on the surface of this film. As Cu^{2+} ions are electrical conductor which help in increasing the mobility of atoms at the surface of film, they may provide novel platform for the use of these films in photovoltaic, sensor, and other device applications.

3.3. FTIR Analysis. Infrared (IR) spectroscopic studies provide useful information about the structure of the compound. IR peak positions as well as their intensities are influenced by the particle size, surface morphology and agglomeration of particles [20]. IR transmittance spectrum of $\text{Zn}_{0.97}\text{Cu}_{0.03}\text{O}$ thick film was recorded in the range of 4000 – $600\ \text{cm}^{-1}$ as presented in Figure 3.

The broad IR transmittance peak observed at $3356\ \text{cm}^{-1}$ is the stretching vibration of hydrogen bonded H_2O and polymeric O-H in Cu-Zn-O lattice [21]. The appearance of this peak shows the adsorption of water in the film from atmospheric moisture and hygroscopic nature of ZnCl_2 precursor. The methylene group ($\nu\ \text{CH}_2$) antisymmetric and symmetric stretching modes are observed at 2916 and $2896\ \text{cm}^{-1}$ in this film spectrum. The absorption peak observed at $2258\ \text{cm}^{-1}$ shows the existence of the CO_2 on the metallic cations [22]. We have also observed transmission peaks around 1624 , 1384 , and $1154\ \text{cm}^{-1}$ pertaining to HOH bending/C=O

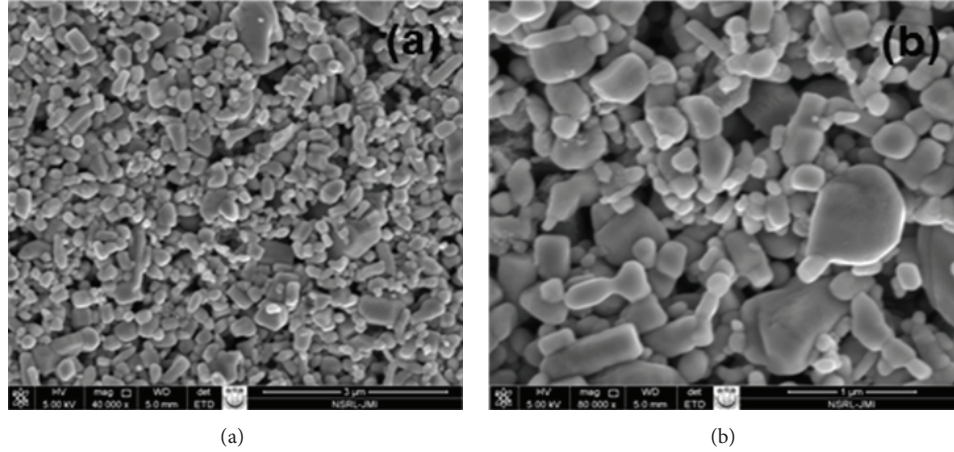


FIGURE 2: SEM images of screen printed Zn_{0.97}Cu_{0.03}O thick film.

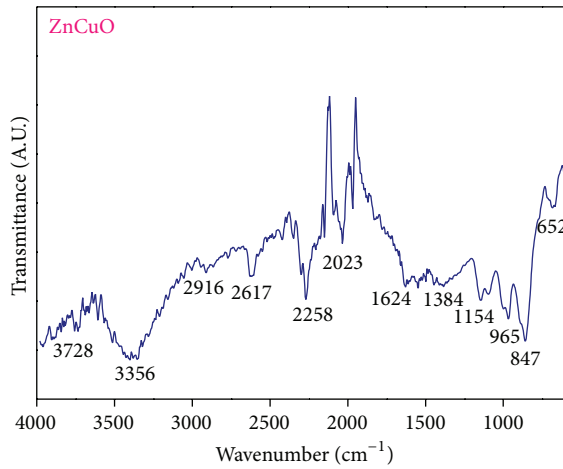


FIGURE 3: IR transmittance spectrum of screen printed Zn_{0.97}Cu_{0.03}O thick film in 4000–600 cm⁻¹ region.

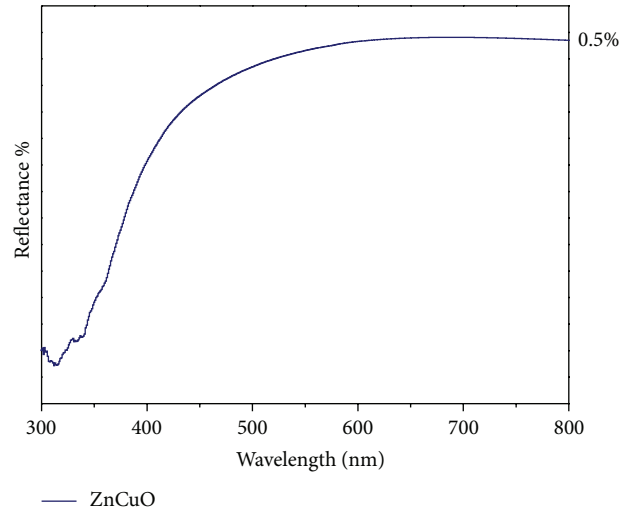


FIGURE 4: UV-VIS spectrum of screen printed Zn_{0.97}Cu_{0.03}O thick film.

stretching mode, C-OH plane bending, and C-OH out-of-plane bending, respectively [23]. The medium intensity bands at 965, 847, and 652 cm⁻¹ are assigned to Cu-O-Zn, Cu-O, and Zn-O stretching modes, respectively. The shift in peak positions to higher wavenumber as compared to pure Cu-O and Zn-O is attributed to the change in crystalline field effect induced by substitution of Cu²⁺ at Zn²⁺ site. IR transmittance peak at 1624 cm⁻¹ appears due to bending mode of H₂O.

3.4. Optical Analysis. Figure 4 shows the UV-visible diffused reflection spectrum of Zn_{0.97}Cu_{0.03}O thick film from which the band gap energy has been calculated by using Kubelka-Munk function [24] which is proportional to α as in (2). Almost all the II–VI compounds are direct band gap semiconductor. The relation between absorption coefficient (α) and incident photon energy ($h\nu$) can be written as [25]

$$\alpha h\nu = A(h\nu - E_g)^{1/2}, \quad (2)$$

where A is constant and E_g is the direct band gap.

The optical band gap of the film is obtained by extrapolation of the linear portion of the graph between the modified Kubelka-Munk function $[F(R)h\nu]^2$ and photon energy ($h\nu$), given by

$$F(R) = \frac{(1 - R)^2}{2R}, \quad (3)$$

where R is the magnitude of the reflectance as function of energy. The direct band gap comes out to be 3.18 eV according to [26] and is shown in Figure 5. This equation is usually applicable for the materials which have high light scattering and absorbing particles in their matrix. Therefore, diffused reflectance is effective for determining the band gap of the solar cell absorbers.

3.5. Electrical Conductivity. Electrical conductivity measurement is very important parameter for understanding the nature and type of material for using them electronic device

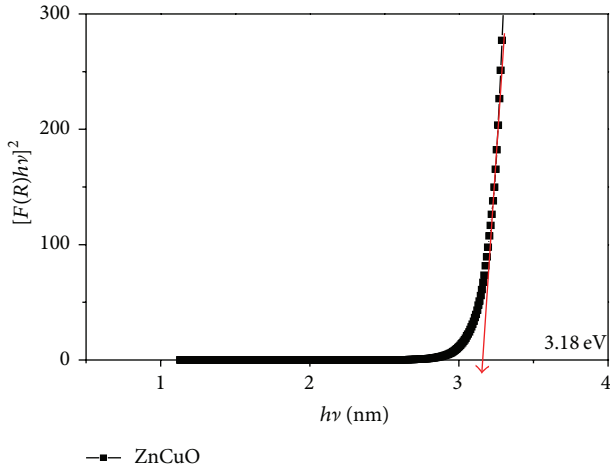


FIGURE 5: Direct band gap energy of screen printed $\text{Zn}_{0.97}\text{Cu}_{0.03}\text{O}$ thick film.

development. Oxides used for thick films are broadly classified into two groups: metallic, where the resistivity obeys a power-law depending on temperature $\rho \propto T^n$, where $n > 0$, and semiconducting where resistivity usually follows the exponential law $\rho \propto \exp(-E/KT)$. The DC electrical conductivity measurements have been carried out in the temperature range 300–400 K. The electrical resistivity (ρ) has been calculated by using [27]

$$\rho = \frac{\pi t}{\ln 2} \left(\frac{V}{I} \right), \quad (4)$$

where ρ is the resistivity ($\Omega\text{-cm}$), t is the sample thickness (cm), V is the applied voltage, and I is the source current (A). The temperature dependency of the DC resistivity can be shown by the well-known Arrhenius equation, given by

$$\rho = \rho_0 \exp\left(-\frac{\Delta E}{KT}\right), \quad (5)$$

where ρ_0 is the preexponential factor, ΔE is the activation energy, K is the Boltzmann constant, and T is the temperature (in Kelvin). The variation of electrical resistivity with temperature for $\text{Zn}_{0.97}\text{Cu}_{0.03}\text{O}$ is shown in Figure 6 indicating the semiconducting nature of the sample because resistivity decreases with increase in operating temperature, thus indicating the negative temperature coefficient of resistance. This must be due to the oxygen deficiency of material in it. When we plot the variation between $\log \rho$ and $10^3/T$, we get activation energy from the slope of the graph that comes out to be 0.66 eV which is in good agreement with the earlier result [15, 28].

4. Conclusion

It has been concluded that screen printing is a versatile technique for preparing alloys of $\text{Zn}_{0.97}\text{Cu}_{0.03}\text{O}$ thick film. The structural, optical, and electrical studies indicate that such types of thick films are suitable for photovoltaic device and other electronic applications. XRD and SEM studies

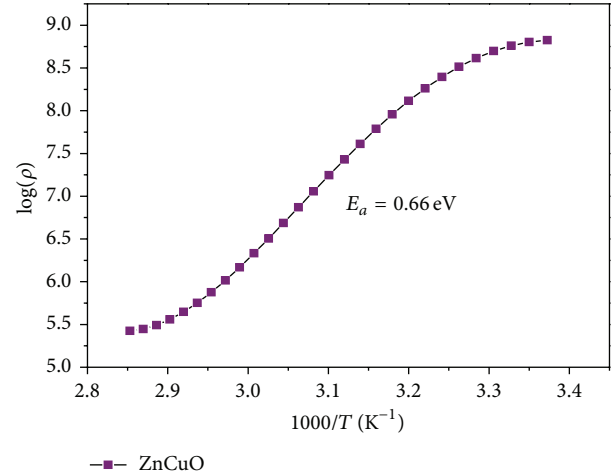


FIGURE 6: Curve between $\log \rho$ and $1000/T$ of screen printed $\text{Zn}_{0.97}\text{Cu}_{0.03}\text{O}$ thick film.

revealed that $\text{Zn}_{0.97}\text{Cu}_{0.03}\text{O}$ films have polycrystalline nature with hexagonal structure. From UV-study direct energy band gap transition has been confirmed and it comes out to be 3.18 eV. FTIR spectroscopy confirmed the incorporation of Cu^{2+} in ZnO lattice. The dark DC resistivity reveals the semiconducting nature of films and gives activation energy value 0.66 eV; this shows that the conduction process of charge carriers is thermally activated. Thus, screen printing is cost effective and user friendly technique and can be used to fabricate polycrystalline thick films having good stability and significant value of activation energy. These films are suitable for solar cells as well as other sensing devices.

Conflict of Interests

The authors declare that there is no conflict of interests regarding the publication of this paper.

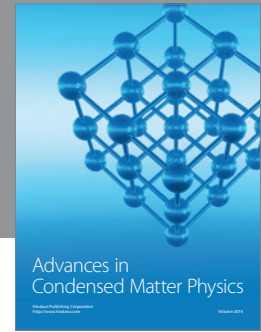
Acknowledgment

The author R. A. Zargar is very thankful to Material Science Research Group at Jamia Millia Islamia and CSIR-NPL, New Delhi, for providing the characterization support to pursue this small piece of work.

References

- [1] X. H. Wang, B. Yao, Z. P. Wei et al., "Acceptor formation mechanisms determination from electrical and optical properties of p-type ZnO doped with lithium and nitrogen," *Journal of Physics D: Applied Physics*, vol. 39, no. 21, pp. 4568–4571, 2006.
- [2] A. Krtschil, A. Dadgar, N. Oleynik, J. Bläsing, A. Diez, and A. Krost, "Local p-type conductivity in zinc oxide dual-doped with nitrogen and arsenic," *Applied Physics Letters*, vol. 87, no. 26, Article ID 262105, 3 pages, 2005.
- [3] W. Lee, R. P. Dwivedi, C. Hong, H. W. Kim, N. Cho, and C. Lee, "Enhancement of the electrical properties of Al-doped ZnO films deposited on ZnO-buffered glass substrates by using an

- ultrathin aluminum underlayer," *Journal of Materials Science*, vol. 43, no. 3, pp. 1159–1161, 2008.
- [4] A. Kassis and M. Saad, "Fill factor losses in ZnO/CdS/CuGaSe₂ single-crystal solar cells," *Solar Energy Materials and Solar Cells*, vol. 80, no. 4, pp. 491–499, 2003.
- [5] H. Kim, A. Piqué, J. S. Horwitz et al., "Effect of aluminum doping on zinc oxide thin films grown by pulsed laser deposition for organic light-emitting devices," *Thin Solid Films*, vol. 377–378, pp. 798–802, 2000.
- [6] K. Rekha, M. Nirmala, M. G. Nair, and A. Anukalini, "Structural, optical, photocatalytic and antibacterial activity of zinc oxide and manganese doped zinc oxide nanoparticles," *Physica B: Condensed Matter*, vol. 405, no. 15, pp. 3180–3185, 2010.
- [7] M. S. Wagh, G. H. Jain, D. R. Patil, S. A. Patil, and L. A. Patil, "Modified zinc oxide thick film resistors as NH₃ gas sensor," *Sensors and Actuators B: Chemical*, vol. 115, no. 1, pp. 128–133, 2006.
- [8] J. C. Fan, K. M. Sreekanth, Z. Xie, S. L. Chang, and K. V. Rao, "p-Type ZnO materials: theory, growth, properties and devices," *Progress in Materials Science*, vol. 58, no. 6, pp. 874–985, 2013.
- [9] K. Samanta, P. Battacharya, and R. S. Katiyar, "Microstructural and ferromagnetic properties of Zn_{1-x}Cu_xO thin films," *Journal of Applied Physics*, vol. 105, no. 11, Article ID 113929, 4 pages, 2009.
- [10] A. Mosbah and M. S. Aida, "Influence of deposition temperature on structural, optical and electrical properties of sputtered Al doped ZnO thin films," *Journal of Alloys and Compounds*, vol. 515, pp. 149–153, 2012.
- [11] S. Muthukumaran and R. Gopalakrishnan, "Structural, FTIR and photoluminescence studies of Cu doped ZnO nanopowders by co-precipitation method," *Optical Materials*, vol. 34, no. 11, pp. 1946–1953, 2012.
- [12] R. A. Michaels, "Emergency planning and the acute toxic potency of inhaled ammonia," *Environmental Health Perspectives*, vol. 107, no. 8, pp. 617–627, 1999.
- [13] D. F. Shriver and P. W. Atkins, *Inorganic Chemistry*, Oxford University Press, 3rd edition, 2004.
- [14] V. Kumar, K. L. A. Khan, G. Singh, T. P. Sharma, and M. Hussain, "ZnSe sintered films: growth and characterization," *Applied Surface Science*, vol. 253, no. 7, pp. 3543–3546, 2007.
- [15] B. Ismail, M. Abaab, and B. Rezig, "Structural and electrical properties of ZnO films prepared by screen printing technique," *Thin Solid Films*, vol. 383, no. 1–2, pp. 92–94, 2001.
- [16] V. Kumar, D. K. Dwivedi, and P. Agrawal, "Optical, structural and electrical properties of nanosized zinc oxide sintered films for photovoltaic applications," *Science of Sintering*, vol. 45, no. 1, pp. 13–19, 2013.
- [17] D. Raoufi and T. Raoufi, "The effect of heat treatment on the physical properties of sol-gel derived ZnO thin films," *Applied Surface Science*, vol. 255, no. 11, pp. 5812–5817, 2009.
- [18] B. D. Cullity, *Elements of X-Ray Diffractions*, Addison-Wesley, Reading, Mass, USA, 1978.
- [19] S. Krishnan, R. Joshi, P. K. Sekhar, and S. Bhansali, "Nanocrystalline palladium thin films for hydrogen sensor application," *Sensor Letters*, vol. 7, no. 1, pp. 31–37, 2009.
- [20] L. Wu, Y. Wu, Y. Shi, and H. Wei, "Synthesis of ZnO nanorods and their optical absorption in visible-light region," *Rare Metals*, vol. 25, no. 1, pp. 68–73, 2006.
- [21] K. Nakamoto, *Infrared and Raman Spectra of Inorganic and Coordination Compounds, Part-A and B*, John Wiley & Sons, New York, NY, USA, 1997.
- [22] J. Das, I. R. Evans, and D. Khushalani, "Zinc glycolate: a precursor to ZnO," *Inorganic Chemistry*, vol. 48, no. 8, pp. 3508–3510, 2009.
- [23] S. Senthilkumaar, K. Rajendran, S. Banerjee, T. K. Chini, and V. Sengodan, "Influence of Mn doping on the microstructure and optical property of ZnO," *Materials Science in Semiconductor Processing*, vol. 11, no. 1, pp. 6–12, 2008.
- [24] P. Kubelka and F. Munk, "Ein Beitrag zur Optik der Farbanstriche," *Zeitschrift fur Technische Physik*, vol. 12, pp. 593–595, 1931.
- [25] J. Tauc, Ed., *Amorphous and Liquid Semiconductors*, Plenum Press, New York, NY, USA, 1974.
- [26] A. E. Morales, E. S. Mora, and U. Pal, "Use of diffuse reflectance spectroscopy for optical characterization of unsupported nanostructures," *Revista Mexicana de Física*, vol. 53, pp. 18–22, 2007.
- [27] "Four-Point Probe Manual, EECS143," Micro fabrication Technology.
- [28] Y. H. Kim, H. Kawamura, and M. Nawata, "The effect of Cr₂O₃ additive on the electrical properties of ZnO varistor," *Journal of Materials Science*, vol. 32, no. 6, pp. 1665–1670, 1997.



Hindawi

Submit your manuscripts at
<http://www.hindawi.com>

